JOC Article

A New Series of *N*-[2,4-Dioxo-6-D-ribitylamino-1,2,3,4-tetrahydropyrimidin-5-yl]oxalamic Acid Derivatives as Inhibitors of Lumazine Synthase and Riboflavin Synthase: Design, Synthesis, Biochemical Evaluation, Crystallography, and Mechanistic Implications

Yanlei Zhang,[†] Boris Illarionov,[‡] Ekaterina Morgunova,[§] Guangyi Jin,[†] Adelbert Bacher,[‡] Markus Fischer,[||] Rudolf Ladenstein,[§] and Mark Cushman*[,†]

Department of Medicinal Chemistry and Molecular Pharmacology, School of Pharmacy and Pharmaceutical Sciences, and The Purdue Cancer Center, Purdue University, West Lafayette, Indiana 47907, Lehrstuhl für Biochemie, Technische Universität München, Lichtenbergstr 4, D-85747 Garching, Germany, Institute of Biochemistry and Food Chemistry, Food Chemistry Division, University of Hamburg, D-20146 Hamburg, Germany, and Karolinska Institute, NOVUM, Center of Bioscience, S-14157 Huddinge, Sweden

cushman@pharmacy.purdue.edu

Received December 11, 2007

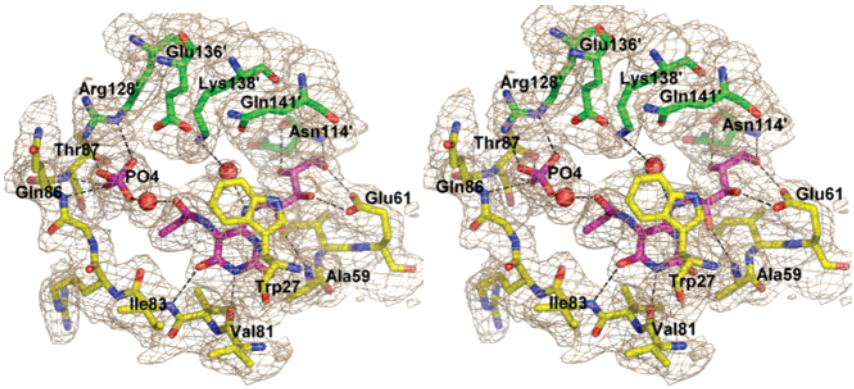

The penultimate step in the biosynthesis of riboflavin is catalyzed by lumazine synthase. Three metabolically stable analogues of the hypothetical intermediate proposed to arise after phosphate elimination in the lumazine synthase-catalyzed reaction were synthesized and evaluated as lumazine synthase inhibitors. All three intermediate analogues were inhibitors of *Mycobacterium tuberculosis* lumazine synthase, *Bacillus subtilis* lumazine synthase, and *Schizosaccharomyces pombe* lumazine synthase, while one of them proved to be an extremely potent inhibitor of *Escherichia coli* riboflavin synthase with a K_i of 1.3 nM. The crystal structure of *M. tuberculosis* lumazine synthase in complex with one of the inhibitors provides a model of the conformation of the intermediate occurring immediately after phosphate elimination, supporting a mechanism in which phosphate elimination occurs before a conformational change of the Schiff base intermediate toward a cyclic structure.

Introduction

Riboflavin plays an indispensable role in the maintenance of life through its participation in essential electron-transport processes. While vertebrates obtain riboflavin from dietary sources, pathogenic microorganisms acquire it through biosynthesis. A variety of Gram-negative Enterobacteria as well as *Candida*- and *Saccharomyces*-type yeasts lack an efficient riboflavin uptake system and are therefore dependent on their own endogenous biosynthesis mechanisms to secure the vitamin.[1−4] Since a clear rationale for selective toxicity to the

[†] Purdue University.
[‡] Technische Universität München.
[§] Karolinska Institute.
[||] University of Hamburg.

10.1021/jo702631a CCC: $40.75
Published on Web 03/11/2008

pathogen and not the host can be advanced, the enzymes in the riboflavin biosynthesis pathway are attractive targets for the design and synthesis of new antibiotics. In fact, expression of the *Salmonella* riboflavin biosynthesis gene *ribB* has recently been shown to play an essential role in enteritis induction and systemic typhoid fever animal disease models.[5,6]

Increasing bacterial resistance to the known antibiotics has seriously compromised their efficacy, and it is therefore prudent for the medical scientific community to discover and develop new types of antibiotics. The present communication focuses on the last two enzymes in the riboflavin biosynthesis pathway, lumazine synthase and riboflavin synthase. Lumazine synthase catalyzes the condensation of 5-amino-6-D-ribitylamino-2,4-(1*H*,3*H*)-pyrimidinedione (**1**) with 3,4-dihydroxybutanone 4-phosphate (**2**) to afford 6,7-dimethyl-8-D-ribityllumazine (**3**).[7,8] Riboflavin synthase catalyzes a mechanistically unusual dismutation of two molecules of **3** to form one molecule of riboflavin (**4**) and one molecule of the lumazine synthase substrate **1** (Scheme 1).[9−13]

A mechanism of the riboflavin synthase-catalyzed dismutation reaction is outlined in Scheme 2. Intermediates **5** and **6** are derived by deprotonation of the C-7 methyl group of one substrate molecule **3** and addition of an undefined nucleophile X^- to the C-7 carbon of a second molecule of **3**.[14−16] Although the identity of the nucleophile has not been rigorously established, likely candidates include water or one of the ribityl hydroxyl groups.[17,18] Nucleophilic attack of the carbanion **5** on the imine **6** would afford intermediate **7**, which could tautomerize to afford compounds **8** and then **9**. Elimination of "X^-" would lead to the iminium ion **10**, which could undergo intramolecular nucleophilic attack by the enamine to afford the intermediate **11**. The pentacyclic compound **11** has been isolated and shown to be a kinetically competent intermediate, and its structure has been established by multinuclear NMR spectroscopy.[11] Two sequential elimination reactions would then produce

SCHEME 1. Last Two Steps in the Riboflavin Biosynthesis Pathway

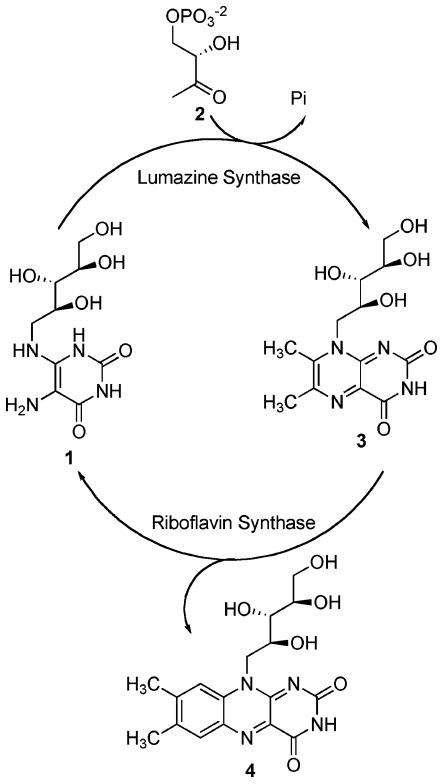

the final products **1** and **4**. The reaction mechanism shown in Scheme 2 is essentially the same as that proposed earlier,[11] except it involves the iminium ion **10** instead of a direct displacement of "X^-" by the enamine in intermediate **9**.

The details of the reaction catalyzed by lumazine synthase have not been completely elucidated. The mechanism outlined in Scheme 3 involves the condensation of the primary amino group of the substituted pyrimidinedione **1** with the ketone **2** to give Schiff base **13**, elimination of phosphate to yield the enol **14**, tautomerization of the enol **14** and isomerization of the imine to produce the ketone **15**, ring closure, and dehydration of the covalent hydrate **16** to provide the product **3**.[19] It can be assumed that the inorganic phosphate formed after elimination from **13** would remain enzyme bound, at least for some time, but that it would eventually have to be removed to make room for another molecule of the substrate **2**.

Although the mechanism outlined in Scheme 3 is certainly very reasonable, the details of the pathway, such as the timing of phosphate elimination relative to the conformational reorganization of the side chain to allow cyclization, and the isomerization of the trans Schiff base to a cis Schiff base, or the possible initial formation of a cis Schiff base, remain unknown.[19] For example, the conformational change of the side chain might occur with the phosphate still covalently bound to form intermediate **17**, which could then eliminate phosphate to generate the enol in **18** close to the ribitylamino group (Scheme 4).[20]

One of the main goals of the present investigation has been to differentiate between the two mechanisms represented in

(1) Wang, A. I. *Chuan Hsueh Pao* **1992**, *19*, 362−368.
(2) Oltmanns, O.; Lingens, F. *Z. Naturforsch.* **1967**, *22 b*, 751−754.
(3) Logvinenko, E. M.; Shavlovsky, G. M. *Mikrobiologiya* **1967**, *41*, 978−979.
(4) Neuberger, G.; Bacher, A. *Biochem. Biophys. Res. Commun.* **1985**, *127*, 175−181.
(5) Rollenhagen, C.; Bumann, D. *Infect. Immun.* **2006**, *74*, 1649−1660.
(6) Becker, D.; Selbach, M.; Rollenhagen, C.; Ballmaier, M.; Meyer, T. F.; Mann, M.; Bumann, D. *Nature* **2006**, *440*, 303−307.
(7) Neuberger, G.; Bacher, A. *Biochem. Biophys. Res. Commun.* **1986**, *139*, 1111−1116.
(8) Kis, K.; Volk, R.; Bacher, A. *Biochemistry* **1995**, *34*, 2883−2892.
(9) Bacher, A.; Eberhardt, S.; Richter, G. In *Escherichia coli and Salmonella: Cellular and Molecular Biology*, 2nd ed.; Neidhardt, F. C., Ed.; ASM Press: Washington, DC, 1996; pp 657−664.
(10) Gerhardt, S.; Schott, A.-K.; Kairies, N.; Cushman, M.; Illarionov, B.; Eisenreich, W.; Bacher, A.; Huber, R.; Steinbacher, S.; Fischer, M. *Structure* **2002**, *10*, 1371−1381.
(11) Illarionov, B.; Eisenreich, W.; Bacher, A. *Proc. Natl. Acad. Sci. U.S.A.* **2001**, *98*, 7224−7229.
(12) Illarionov, B.; Kemter, K.; Eberhardt, S.; Richter, G.; Cushman, M.; Bacher, A. *J. Biol. Chem.* **2001**, *276*, 11524−11530.
(13) Plaut, G. W. E.; Harvey, R. A. *Methods Enzymol.* **1971**, *18B*, 515−538.
(14) Beach, R. L.; Plaut, G. W. E. *J. Am. Chem. Soc.* **1970**, *92*, 2913−2916.
(15) Beach, R. L.; Plaut, G. W. E. *J. Am. Chem. Soc.* **1971**, *36*, 3937−3943.
(16) Paterson, T.; Wood, H. S. C. *J. Chem. Soc., Perkin Trans. 1* **1972**, 1051−1056.
(17) Cushman, M.; Patrick, D. A.; Bacher, A.; Scheuring, J. *J. Org. Chem.* **1991**, *56*, 4603−4608.
(18) Bown, D. H.; Keller, P. J.; Floss, H. G.; Sedlmaier, H.; Bacher, A. *J. Org. Chem.* **1986**, *51*, 2461.
(19) Volk, R.; Bacher, A. *J. Am. Chem. Soc.* **1988**, *110*, 3651−3653.
(20) Zhang, X.; Meining, W.; Cushman, M.; Haase, I.; Fischer, M.; Bacher, A.; Ladenstein, R. *J. Mol. Biol.* **2003**, *328*, 167−182.

SCHEME 2. Hypothetical Mechanism of the Riboflavin Synthase Catalyzed Reaction (X−, Undefined Nucleophile; R, Ribityl Chain)

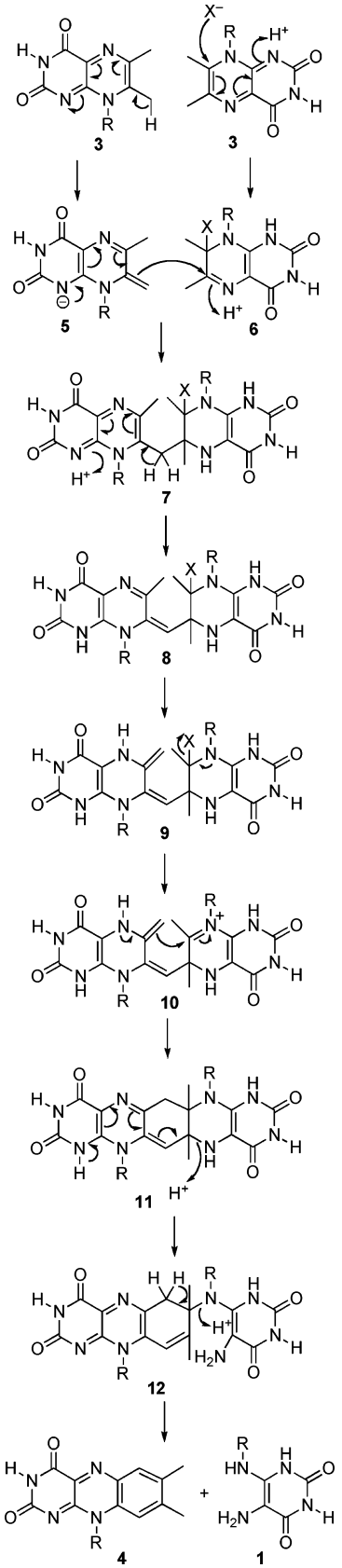

SCHEME 3. Hypothetical Reaction Mechanism of the Lumazine Synthase-Catalyzed Reaction

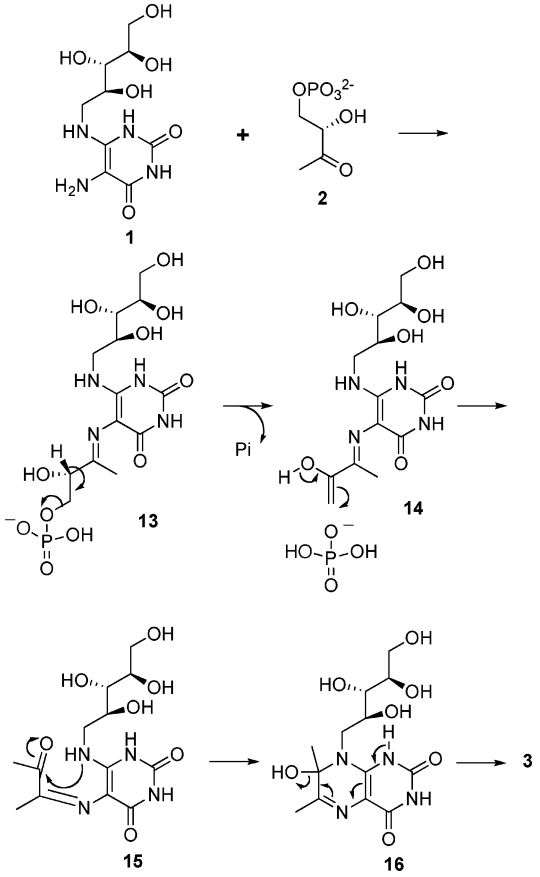

SCHEME 4. Alternative Mechanism of the Lumazine Synthase-Catalyzed Reaction

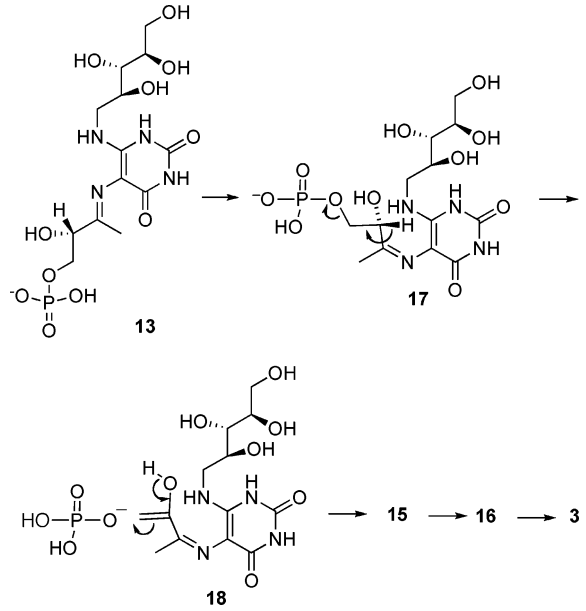

Schemes 3 and 4. In the present case, an attempt was made to synthesize metabolically stable analogues of the hypothetical intermediate **14**, crystallize a lumazine synthase complex with a bound intermediate analogue and bound inorganic phosphate, and determine the structure of the intermediate analogue by crystallography. This would hopefully provide insight into the question of whether a ternary complex consisting of the enzyme, an analogue of **14**, and inorganic phosphate can exist, and if so, the structure of the complex.

SCHEME 5. Synthesis of Fully Protected Ribitylamino-pyrimidinedione 24[a]

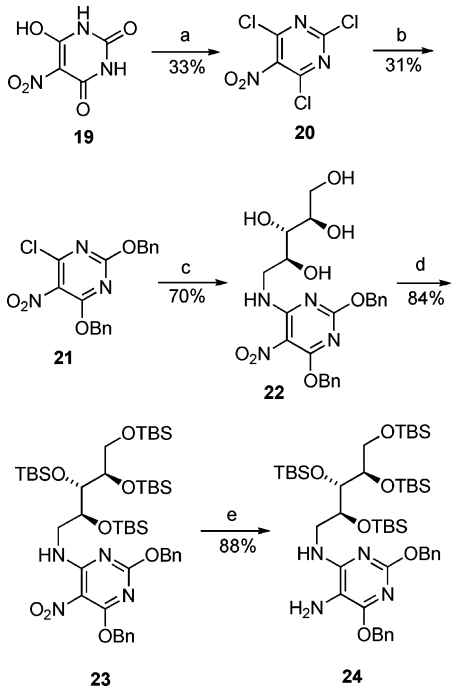

[a] Reagents and conditions: (a) $POCl_3$, diethylaniline, 0 °C (30 min), 23 °C (2 h); (b) BnONa/THF, −20 °C (2 h), 23 °C (4 h); (c) ribitylamine, DMF, rt (2 h); (d) TBS triflate, triethylamine, 23 °C (11 h); (e) $Na_2S_2O_4$, MeOH, H_2O, 90 °C (5.5 h).

Results and Discussion

Synthesis. Lumazine synthase and riboflavin synthase inhibitors that are based on the structures of the hypothetical intermediates in the enzyme-catalyzed reactions are generally very polar molecules, making purification problematic. In the present case, the pyrimidinedione ring was masked with benzyl groups that were cleaved by hydrogenolysis in the final step. By simply removing the catalyst and solvent, the final compounds could be synthesized in good yields and the crude products were fairly pure. In addition, TBS protection of the hydroxyl groups of the ribityl side chain was employed to avoid their reaction during acylation of the primary amino group attached to the pyrimidine ring.

Reaction of 5-nitrobarbituric acid **(19)** with phosphorus oxychloride provided the trichloride **20** (Scheme 5). Nucleophilic aromatic substitution of **20** with sodium benzyl oxide yielded intermediate **21**. A second nucleophilic aromatic substitution with ribitylamine afforded compound **22** in good yield. Due to its poor solubility in organic solvents, the four hydroxyl groups of **22** were protected as their *tert*-butyldimethylsilyl ethers to yield **23**. The nitro group of **23** was then reduced, resulting in the amine **24**. The amine **24** was not stable, and the crude product was used in the next reaction immediately after the solvent was removed.

The key intermediate **24** was reacted with ethyl chlorooxoacetate, isobutyryl chloride, or propionyl chloride to afford the corresponding amides **25**, **28**, and **31** (Scheme 6), which were deprotected with HF-pyridine to yield **26**, **29**, and **32**. Removal of the benzyl protecting groups from **26**, **29**, and **32** by catalytic hydrogenolysis using palladium on carbon provided the desired products **27**, **30**, and **33** in high yield.

Enzyme Kinetics. The hypothetical intermediate analogues **27**, **30**, and **33** were tested as inhibitors of recombinant lumazine synthases from *M. tuberculosis*, *B. subtilis*, and *S. pombe*. Compounds **27**, **30**, and **33** are product **1** analogues of the riboflavin synthase-catalyzed reaction and might therefore be expected to inhibit riboflavin synthase as well. The analogues were therefore also tested for inhibition of recombinant *E. coli* riboflavin synthase.

Representative Lineweaver-Burke plots for inhibition of *M. tuberculosis* lumazine synthase by inhibitors **27**, **30**, and **33** are presented in Figure S26 (Supporting Information). The inhibition constants and inhibition mechanisms for these inhibitors are listed in Table 1. The data reveal that the relative potencies of compounds **27**, **30**, and **33** as inhibitors of lumazine synthase depend entirely on the enzyme species. In the case of *M. tuberculosis* lumazine synthase, the relative potencies increase in the order **33** < **30** < **27**, while in the case of *B. subtilis* lumazine synthase, the order is reversed: **27** < **30** < **33**. With *S. pombe* lumazine synthase, the potencies do not change significantly. In addition, the mechanism of inhibition can be partial, competitive, or mixed depending on the inhibitor and the species of enzyme (Table 1).

The ethyl oxalate derivative **27** proved to be an unusually potent inhibitor of *E. coli* riboflavin synthase, with a K_i of 1.3 nM. The potency and the structure of this compound are reminiscent of the potent 6,7-dihydro-6,7-dioxo-8-ribityllumazine system **34**, which was previously shown to be a potent inhibitor of baker's yeast riboflavin synthase (K_i 25 nM)[21] and *Ashbya gossypii* riboflavin synthase (K_i 9 nM).[22] Evidently, conformational restriction of the 1,2-diketone moiety of **27** in a dioxolumazine system **34** is not required for potent riboflavin synthase inhibitory activity. An antibiotic that could inhibit both riboflavin synthase and lumazine synthase would make it more difficult for a pathogenic microorganism to become resistant, since in order to do so, it would have to mutate both enzymes simultaneously.

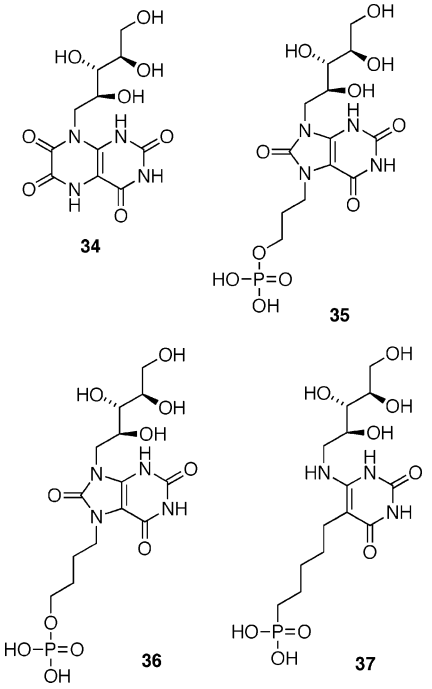

Crystallography. The complex formed from inhibitor **33** and *M. tuberculosis* lumazine synthase was crystallized in sitting

SCHEME 6. Synthesis of Target Compounds 27, 30, and 33[a]

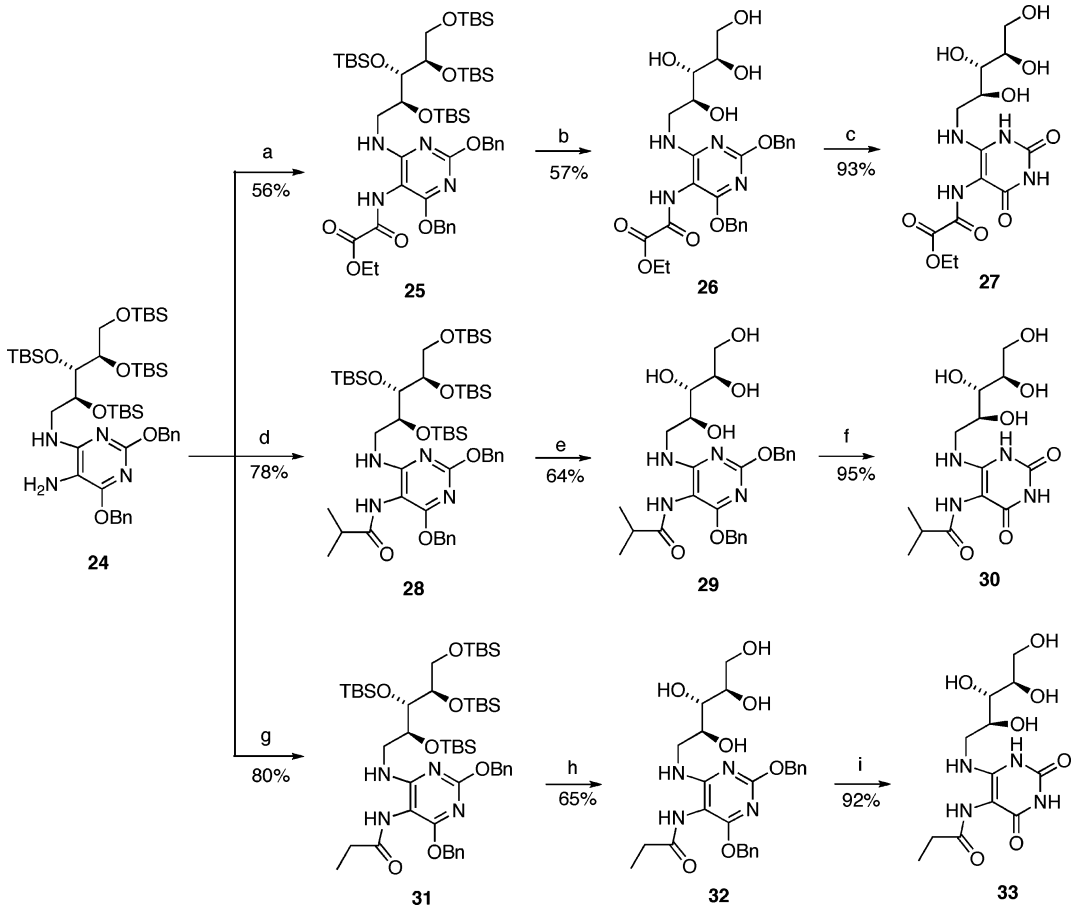

[a] Reagents and conditions: (a) ethyl chlorooxoacetate, triethylamine, THF, 0 °C (30 min), 23 °C (10 min); (b) HF−pyridine, THF, 23 °C (5 h); (c) Pd/C, H_2, MeOH−H_2O, 23 °C (24 h); (d) isobutyryl chloride, triethylamine, THF, 0 °C (40 min), 23 °C (40 min); (e) HF−pyridine, THF, 23 °C (6 h); (f) Pd/C, H_2, MeOH−H_2O, 23 °C (24 h); (g) propionyl chloride, triethylamine, THF, 0 °C (40 min) 23 °C (40 min); (h) HF-pyridine, THF, 23 °C (6 h); (i) Pd/C, H_2, MeOH−H_2O, 23 °C (24 h).

TABLE 1. Inhibition Constants vs Lumazine Synthases from *M. tuberculosis*, *B. subtilis*, *S. pombe*, and Riboflavin Synthase from *E. coli*

compd	parameter	*M. tuberculosis* lumazine synthase[e]	*B. subtilis* lumazine synthase[f]	*S. pombe* lumazine synthase[g]	*E. coli* riboflavin synthase[h]
27	K_s[a] (mM)	53 ± 11	5.4 ± 0.5	1.0 ± 0.1	2.61 ± 0.15
	k_{cat}[b] (min^{-1})	0.11 ± 0.01	2.5 ± 0.1	1.00 ± 0.03	16.3 ± 0.34
	K_i[c] (μM)	4.0 ± 1.7	607 ± 177	1.1 ± 0.2	0.0013 ± 0.0001
	K_{is}[d] (μM)	35 ± 14		15 ± 3	0.34 ± 0.08
	mechanism	partial	competitive	mixed	mixed
30	K_s (μM)	63 ± 8	3.6 ± 0.3	1.1 ± 0.1	5.9 ± 0.6
	k_{cat} (min^{-1})	0.11 ± 0.01	0.40 ± 0.01	0.95 ± 0.02	11.8 ± 0.5
	K_i (μM)	42 ± 16	95 ± 36	7.9 ± 0.8	
	K_{is} (μM)	77 ± 28	64 ± 11		>1000
	mechanism	partial	partial	competitive	uncompetitive
33	K_s (μM)	58 ± 8	3.2 ± 0.3	1.9 ± 0.3	6.3 ± 0.7
	k_{cat} (min^{-1})	0.095 ± 0.005	0.37 ± 0.01	1.3 ± 0.1	12.3 ± 0.1
	K_i (μM)	110 ± 14	20 ± 4	11 ± 1	
	K_{is} (μM)		56 ± 12		>1000
	mechanism	competitive	partial	competitive	uncompetitive

[a] K_s is the substrate dissociation constant for the equilibrium E + S ⇄ ES. [b] K_{cat} is the rate constant for the process ES → E + P. [c] K_i is the inhibitor dissociation constant for the process E + I ⇄ EI. [d] K_{is} is the inhibitor dissociation constant for the process ES + I ⇄ ESI. [e] Recombinant lumazine synthase from *M. tuberculosis*, assay performed in Tris hydrochloride buffer. [f] Recombinant lumazine synthase from *B. subtilis*, assay performed in potassium phosphate buffer. [g] *Recombinant* lumazine synthase from *S. pombe*, assay performed in Tris hydrochloride buffer. [h] *Recombinant* riboflavin synthase from *E. coli*, assay performed in phosphate buffer.

drops by the vapor diffusion technique with a macroseeding procedure as previously reported for compounds **35** and **36**, and the crystal structure was determined (Figure 1).[23] The diffraction data were collected using beamline BM14 at the European Synchrotron Light Source (ESRF, Grenoble, France), and the structure was refined to a resolution of 2.3 Å. The active site of *M. tuberculosis* lumazine synthase is known to be located at the interface between two neighboring subunits in the pentameric

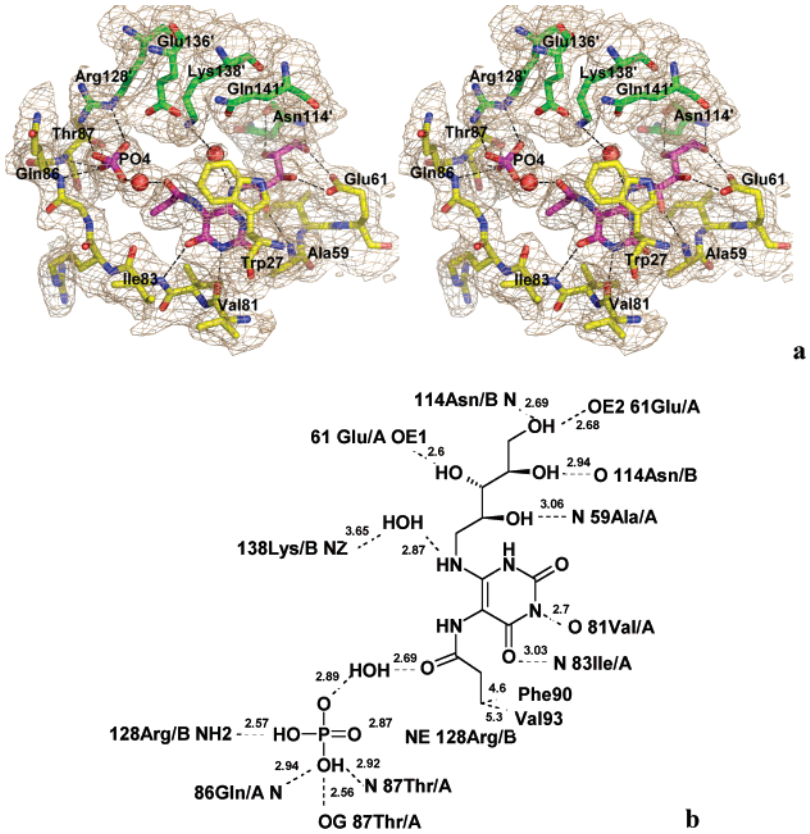

FIGURE 1. Stereodiagram of the 2|Fo|-|Fc| electron density map (σ =1.5) around the active site of *M. tuberculosis* lumazine synthase in complex with inhibitor **33** and phosphate ion (magenta) (a) and the respective schematic drawings of the interactions between the enzyme and the ligand (b). Red spheres indicate water molecules. The carbon atoms of the residues of different subunits are shown in green and in yellow, oxygen atoms are in red, and nitrogen atoms are in blue.

assembly. It is formed by the residues from three β-loops (residues 26−28, 58−61, 81−87) of one subunit as well as residues 128−141 and residue Asn114 of the neighboring subunit.[23] The aromatic ring of the inhibitor **33** is packed in the hydrophobic environment in the active site formed by Trp27, Ile60, Val81 and Val82, Ile83, Phe90, and Val93 residues of one subunit. The pyrimidine ring is in stacking interaction with the indole ring of Trp27 at a distance of 4 Å. This interaction was characterized by a slight deviation of the rings from their parallel positions and was suggested to be weaker in comparison to the previously reported purinetrione inhibitors **35**, **36**, and related purinetriones because of the smaller size of the pyrimidine ring of **33**.[23,24] The terminal methyl group of the inhibitor side chain is directed toward the hydrophobic interior of the pocket and is located at distances of 4.6 and 5.3 Å from the side chains of Phe90 and Val93, respectively. The hydrophobic interaction is supported by two hydrogen bonds formed between the main chain O-Val81 and N3 from the pyrimidine ring and the main chain N-Ala59 and the pyrimidine O2 (Figure 1).

The ribityl chain is embedded in a surface depression formed by residues 56−62 from one subunit and residues 113−114 of the adjacent subunit with seven H-bonds to both subunits in total. A schematic diagram of protein-inhibitor interactions is presented in Figure 1b.

The phosphate ion forms two hydrogen bonds with atoms N and OG of Thr87 with a distance of 2.9 and 2.6 Å, respectively, a hydrogen bond with the main chain nitrogen atom of Gln86 with a distance of 2.9 Å, and two ionic contacts with NE and NH2 of Arg128 with a distance of 2.9 and 2.6 Å, respectively.

Two water molecules were observed in each of the 10 active sites. One water molecule forms a hydrogen-bonding bridge between the amide side chain carbonyl oxygen of the inhibitor and the oxygen of the buffer-derived inorganic phosphate ion. This water molecule has never been observed before in the crystal structures of complexes formed between other inhibitors and lumazine synthase, which may result from the fact that the previously reported inhibitors do not bear a carbonyl oxygen at the position of the amide carbonyl present in compound **33**. Also, none of the previous crystal structures display the enzyme bound to both an inorganic phosphate and a C-5 pyrimidinedione side chain resembling intermediates **14** and **15**.[10,23−29] Obvi-

(21) Al-Hassan, S. S.; Kulick, R. J.; Livingston, D. B.; Suckling, C. J.; Wood, H. C. S.; Wrigglesworth, R.; Ferone, R. *J. Chem. Soc., Perkin Trans. 1* **1980**, 2645−2656.
(22) Winestock, C. H.; Aogaichi, T.; Plaut, G. W. E. *J. Biol. Chem.* **1963**, *238*, 2866−2874.
(23) Morgunova, K.; Meining, W.; Illarionov, B.; Haase, I.; Jin, G.; Bacher, A.; Cushman, M.; Fischer, M.; Ladenstein, R. *Biochemistry* **2005**, *44*, 2746−2758.
(24) Morgunova, E.; Illarionov, B.; Sambaiah, T.; Haase, I.; Bacher, A.; Cushman, M.; Fischer, M.; Ladenstein, R. *FEBS J.* **2006**, *273*, 4790−4804.
(25) Ladenstein, R.; Meyer, B.; Huber, R.; Labischinski, H.; Bartels, K.; Bartunik, H.-D.; Bachman, L.; Ludwig, H. C.; Bacher, A. *J. Mol. Biol.* **1986**, *187*, 87−100.
(26) Ladenstein, R.; Schneider, M.; Huber, R.; Bartunik, H. D.; Wilson, K.; Schott, K.; Bacher, A. *J. Mol. Biol.* **1988**, *203*, 1045−1070.
(27) Schott, K.; Ladenstein, R.; König, A.; Bacher, A. *J. Biol. Chem.* **1990**, *265*, 12686−12689.
(28) Zhang, X.; Meining, W.; Fischer, M.; Bacher, A.; Ladenstein, R. *J. Mol. Biol.* **2001**, *306*, 1099−1114.
(29) Persson, K.; Schneider, G.; Jordan, D. B.; Viitanen, P. V.; Sandalova, T. *Protein Sci.* **1999**, *8*, 2355−2365.

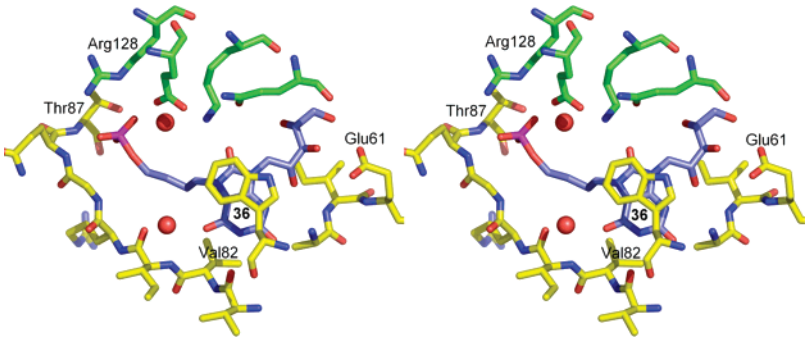

FIGURE 2. Stereoview of the substrate binding site of LS from *M. tuberculosis* with bound purinetrione inhibitor **36**. The inhibitor is shown in blue and magenta (phosphate group), and amino acids interacting with compound are shown in yellow and green. The diagram is programmed for walleyed (relaxed) viewing.

ously, the water molecule occupies an energetically favorable position due to its presence in a hydrogen bond network between the phosphate ion and the inhibitor molecule, which stabilizes the position of the inhibitor. Its presence is significant because it suggests that it may be present and participate in the enzyme-catalyzed reaction. The following are possible roles of this water molecule during catalysis: (1) it may be involved in hydrolysis of the phosphate to form a 1,2-diol that then eliminates water to generate the enol **14**. This seems unattractive because the phosphate is a better leaving group than a hydroxide or water. (2) It could participate as a proton acceptor from carbon during the phosphate elimination reaction. (3) It could stabilize the inorganic phosphate formed after the elimination reaction by hydrogen bonding. (4) It could act as a hydrogen donor or acceptor during tautomerization of the enol **14** to the ketone **15**. (5) Finally, it could stabilize the enol and keto structures during the conformational reorganization of the side chain toward a cyclic structure (**14** → **15**).

One of the goals of the present study was to gain insight into the question of whether phosphate elimination occurs before or after the conformational change toward a cyclic structure (Schemes 3 vs 4). The crystal structure displayed in Figure 1 provides, for the first time, evidence for an extended conformation of the C-5 side chain with inorganic phosphate in the phosphate-binding site of the enzyme. It provides a model of the hypothetical intermediate **14** that would result from phosphate elimination while phosphate remains bound in the phosphate-binding site. Our previously published crystal structure of the phosphonate **37** bound to *S. cerevisiae* lumazine synthase provides a snapshot of the bound hypothetical intermediate **13** formed from the substrates **1** and **2** (Scheme 3).[30] Crystal structures are also available of an analogue of the substrate **1** bound to *B. subtilis* lumazine synthase in which the primary amino group of the substrate **1** is replaced by a nitro group.[26,27]

The second water molecule found in the active site hydrogen bonds to the Lys138 amino group of the enzyme as well as the ribitylamino group of the inhibitor. The oxygen atom of this water molecule mimics the carbonyl oxygen in the five-membered ring of the purinetrione inhibitors, including compounds **35** and **36** (Figure 2). This water molecule likely plays a role that is similar to the carbonyl oxygen in the five-membered ring of the purinetrione inhibitors.

Overall, the evidence provided by the crystal structure shown in Figure 1 supports elimination of the phosphate before the C-5 side chain rotates toward a cyclic structure (Scheme 3). Additional studies will be required to clarify exactly how the substrate **2** displaces inorganic phosphate from the phosphate-binding site of the enzyme during catalysis. Presumably, the binding free energy of the substrate **2** is larger than that of an inorganic phosphate. Crystallization of lumazine synthase in complex with bound organic phosphonate inhibitors (e.g., **37**), as well as isothermal titration calorimetry and crystallization of lumazine synthase with bound organic phosphate inhibitors (e.g., **35** and **36**, Figure 2), have been carried out in phosphate buffer. In these studies, the inhibitors were able to displace inorganic phosphate from its binding site, so it is reasonable to expect that the substrate **2** can as well.[23,24,30,31]

Experimental Section

2,4,6-Trichloro-5-nitropyrimidine (20). 5-Nitrobarbituric acid (3.02 g, 17.48 mmol) was added to fresh $POCl_3$ (18 mL) in a dry flask. Diethylaniline (12.50 g, 83.9 mmol) was added dropwise while the mixture was cooled with an ice bath. The speed of DEA dropping was roughly one drop per second. After addition was complete, the reaction mixture was stirred for 0.5 h on the ice bath. The ice bath was removed, and the reaction mixture was stirred at 23 °C for 2 h and then poured slowly into ice−water to quench the reaction. During this process, the temperature was kept below 5 °C. After all of the reaction mixture had been poured into ice−water, the solution was stirred at 23 °C for a few min until it reached 23 °C. The solution was extracted with ethyl ether (4 × 35 mL), and the ether layer was washed with water (2 × 10 mL) and dried with Na_2SO_4. The ether solution was concentrated to yield a residue that was extracted with boiling hexane (4 × 70 mL). The extracts were combined and the solvent was removed to afford the product (1.31 g, 33%) as a yellow powder: mp 56−58 °C (lit.[32] mp 57−58 °C).

2,4-Bis(benzyloxy)-6-chloro-5-nitropyrimidine (21). NaH (0.276 g, 11.5 mmol) was added to the solution of benzyl alcohol (1.24 g, 11.5 mmol) in THF (26 mL) at 23 °C, and the mixture was stirred for 30 min. The solution was added dropwise into a solution of compound **20** (1.31 g, 5.75 mmol) in THF (26 mL) at −20 °C. The reaction mixture was stirred at −20 °C for 2 h and at 23 °C for 4 h. A few drops of acetic acid were added to stop the reaction. The reaction mixture was concentrated in vacuo, and the residue was extracted with ether. The extracts were combined, and solvent was removed. The residue was separated by silica gel TLC with CH_2Cl_2−hexane 1:1 as the mobile phase to provide the product **21**[33] (667 mg, 31.3%) as yellow crystals: mp 105−107 °C; ^{1}H

(30) Meining, W.; Mörtl, S.; Fischer, M.; Cushman, M.; Bacher, A.; Ladenstein, R. *J. Mol. Biol.* **2000**, *299*, 181−197.
(31) Morgunova, E.; Saller, S.; Haase, I.; Cushman, M.; Bacher, A.; Fischer, M.; Ladenstein, R. *J. Biol. Chem.* **2007**, *282*, 17231−17241.
(32) Robins, R. K.; Dille, K. L.; Christensen, B. E. *J. Org. Chem.* **1954**, *19*, 930−933.
(33) Hashizume, K.; Inoue, S. *Yakagaku Zasshi* **1985**, *105*, 362−367.

NMR (300 MHz, $CDCl_3$) δ 7.61−7.50 (m, 10 H), 5.65 (s, 2 H), 5.59 (s, 2 H); ^{13}C NMR (75 MHz, $CDCl_3$) δ 164.6, 163.3, 155.0, 136.0, 135.4, 130.0, 129.6, 129.2, 72.0, 71.7; ESIMS *m*/*z* 394 (MNa^+).

2-Benzyloxy-5-nitro-4,6-bis(ribitylamino)pyrimidine (22). Compound **21** (539 mg, 1.45 mmol) and ribitylamine (548 mg, 3.63 mmol) were added to DMF (8 mL). The reaction mixture was stirred at 23 °C for 2 h. DMF was removed in vacuo. The residue was separated by silica gel flash chromatography with $CHCl_3$−methanol 3:1 as the mobile phase to afford the product as an amorphous white powder (488 mg, 70%): ^{1}H NMR (300 MHz, DMSO-d_6) δ 9.08 (s, 1 H), 7.49−7.31 (m, 10 H), 5.50 (s, 2 H), 5.41 (s, 2 H), 5.03−5.02 (d, J = 5.3 Hz, 1 H), 4.70−4.68 (d, J = 4.9 Hz, 1 H), 4.43−4.40 (t, J = 5.5 Hz, 1 H), 3.91−3.85 (m, 2 H), 3.61−3.30 (m, 5 H); ^{13}C NMR (75 MHz, DMSO-d_6) δ 165.9, 162.4, 158.3, 136.0, 135.9, 128.5, 128.3, 128.0, 127.5, 112.0, 73.5, 72.7, 69.3, 69.2, 69.0, 63.2, 44.0, 40.3, 40.1, 39.8, 39.2, 38.9, 38.7; ESIMS *m*/*z* 487 (MH^+). Anal. Calcd for $C_{23}H_{26}N_4O_8$: C, 56.79; H, 5.39; N, 11.52. Found: C, 56.50; H, 5.42; N, 11.33.

2,4-Bis(benzyloxy)-5-nitro-6-[2,3,4,5-tetrakis-(*O*-*tert*-butyldimethylsilanyl)ribitylamino]pyrimidine (23). Compound **22** (243 mg, 0.5 mmol) and TBS triflate (792 mg, 3 mmol) were added into a flask. Triethylamine (7.74 mL) was added to the flask to make a solution. The reaction mixture was stirred at 23 °C for 11 h. The TEA was removed in vacuo. The residue was added to ethyl acetate (12.8 mL), and the mixture was stirred for 2 h at 23 °C. The cloudy ethyl acetate solution was filtered through Celite to afford a clear solution. The solvent was evaporated, and the residue was separated by silica gel flash chromatography (hexane−ethyl acetate 95:5) to provide the product **23** as a yellow oil (396 mg, 84%): ^{1}H NMR (300 MHz, $CDCl_3$) δ 8.96 (s, 1 H), 7.48−7.27 (m, 10 H), 5.51 (s, 2 H), 5.44−5.31 (q, J = 12 Hz, 2 H), 4.14−4.09 (m, 1 H), 3.99−3.89 (m, 2 H), 3.85−3.82 (m, 1 H), 3.73−3.69 (m, 1 H), 3.57−3.52 (m, 2 H), 0.88−0.85 (m, 36 H), 0.11−0.04 (m, 24 H); ESIMS *m*/*z* 944 (MH^+). Anal. Calcd for $C_{47}H_{82}N_4O_8Si_4$: C, 59.83; H, 8.76; N, 5.94. Found: C, 59.78; H, 8.67; N, 5.76.

5-Amino-2,4-bis(benzyloxy)-6-[2,3,4,5-tetrakis-*O*-(*tert*-butyldimethylsilanyl)ribityl]pyrimidine (24). Compound **23** (47 mg, 0.05 mmol) was added to a vial. Methanol (1 mL) and water (0.1 mL) were added to the vial. $Na_2S_2O_4$ (66 mg, 0.38 mmol) was added to the reaction mixture. The reaction mixture was stirred for 5.5 h at 90 °C in a sealed vial and then cooled to 23 °C. The solution was filtered through Celite, and the filtrate was dried to afford a residue. The residue was separated by silica gel flash chromatography with hexane−ethyl acetate 20:1 as mobile phase to afford the product as a yellow oil (40 mg, 87.5%): ^{1}H NMR (300 MHz, $CDCl_3$) δ 7.37−7.16 (m, 10 H), 5.26−5.23 (m, 4 H), 3.90−3.65 (m, 7 H), 0.83−0.81 (m, 36 H), 0.048 − −0.041 (m, 24 H); ESIMS *m*/*z* 914 (MH^+).

***N*-{2,4-Bis(benzyloxy)-6-[2,3,4,5-tetrakis-*O*-(*tert*-butyldimethylsilanyl)ribitylamino]-pyrimidin-5-yl}oxalamic Acid Ethyl Ester (25).** Compound **24** (40 mg, 0.044 mmol) was mixed with THF (1 mL), and then TEA (40 mg, 0.4 mmol) was added to the THF solution. The mixture was cooled to 0 °C, and ethyl chlorooxoacetate (7.4 μL, 9 mg, 0.066 mmol) was added dropwise. The reaction mixture was stirred at 0 °C for 0.5 h. The reaction mixture was warmed to 23 °C and stirred for 10 min. The mixture was evaporated in vacuo to yield a residue that was purified by silica gel flash chromatography (hexane−ethyl acetate 10:1) to provide the product as a viscous yellow oil (25 mg, 56%): ^{1}H NMR (300 MHz, $CDCl_3$) δ 8.12 (s, 1 H), 7.38−7.20 (m, 10 H), 5.43−5.22 (m, 4 H), 4.34−4.27 (q, J = 6 Hz, 2 H), 3.94−3.48 (m, 7 H), 1.36−1.31 (t, J = 7 Hz, 3 H) 0.83−0.81 (m, 36 H), 0.06−0.06 (m, 24 H); ^{13}C NMR (75 MHz, $CDCl_3$) δ 163.8, 162.2, 160.0, 159.5, 154.7, 136.8, 136.4, 128.3, 128.2, 128.0, 127.8, 127.7, 127.6, 92.9, 76.6, 74.5, 71.4, 68.8, 68.2, 64.4, 63.2, 43.1, 26.0, 25.9, 25.8, 18.3, 18.2, 18.1, 17.9, 13.9, −4.1, −4.4, −4.7, −5.9, −5.7, −5.5; IR ($CDCl_3$, film) 2955, 2930, 2886, 1800, 1763, 1610, 1514, 1472, 1395, 1375, 1251, 1228 cm^{-1}; MALDIMS *m*/*z* 1013 (MH^+). Anal. Calcd for $C_{51}H_{88}N_4O_9Si_4$: C, 60.43; H, 8.75; N, 5.53. Found: C, 60.31; H, 8.56; N, 5.37.

***N*-[2,4-Bis(benzyloxy)-6-(ribitylamino)pyrimidin-5-yl]oxalamic Acid Ethyl Ester (26).** Compound **25** (35 mg, 0.034 mmol) was added to THF (1 mL). HF·Py (0.4 mL) was added to the THF solution. The reaction mixture was stirred for 5 h at 23 °C. Saturated $NaHCO_3$ solution was added to the reaction mixture to neutralize it to pH = 8. The solution was extracted with chloroform, and the extracts were combined and dried over Na_2SO_4. The chloroform solution was evaporated and the residue was separated by TLC to afford compound **26** (11 mg, 57%) as an oil: ^{1}H NMR (300 MHz, $CDCl_3$) δ 8.73 (s, 1 H), 7.52−7.39 (m, 10 H), 6.35 (s, 1 H), 5.56 (s, 2 H), 5.43 (s, 2 H), 4.45−4.38 (q, J = 7 Hz, 2 H), 3.92−3.81 (m, 5 H), 3.69−3.63 (m, 2 H), 1.46−1.42 (t, J = 6 Hz, 3 H); ^{13}C NMR (75 MHz, $CDCl_3$) δ 164.7, 162.4, 160.8, 160.4, 156.4, 136.8, 128.9, 128.4, 128.3, 128.1, 92.8, 74.0, 73.7, 71.7, 69.6, 68.9, 64.1, 63.8, 44.3, 14.2; MALDIMS *m*/*z* 557 (MH^+). Anal. Calcd for $C_{27}H_{32}N_4O_9$·0.4 H_2O: C, 57.52; H, 5.86; N, 9.94. Found: C, 57.78; H, 5.79; N, 9.58.

***N*-[2,4-Dioxo-6-(ribitylamino)-1,2,3,4-tetrahydropyrimidin-5-yl]oxalamic Acid Ethyl Ester (27).** Starting material **26** (11 mg, 0.020 mmol) and Pd/C (10%, 2.5 mg) were added into a flask. Methanol−water (2.5 mL-0.25 mL) was added, and the reaction mixture was stirred under H_2 for 24 h. The reaction mixture was filtered, and the filtrate was evaporated to provide the product **27** (6.9 mg, 93%) as a white semisolid powder: ^{1}H NMR (300 MHz, D_2O) δ 4.18−4.11 (q, J = 7 Hz, 2 H), 3.67−3.24 (m, 7 H), 1.13−1.08 (t, J = 7 Hz, 3 H); ^{13}C NMR (D_2O) (75 MHz) δ 162.5, 160.1, 153.7, 151.6, 85.4, 72.6, 72.5, 70.8, 64.6, 62.7, 44.6, 13.4; ESI *m*/*z* 579 (MNa^+). Anal. Calcd for $C_{13}H_{20}N_4O_9$·0.4H_2O: C, 39.85; H, 5.58; N, 14.29. Found: C, 39.84, H, 5.50, N, 14.72.

***N*-(2,4-Bis(benzyloxy)-6-[2,3,4,5-(*tert*-butyldimethylsilyl)ribitylamino]pyrimidin-5-yl)isobutyramide (28).** Compound **23** (600 mg, 0.636 mmol) was dissolved in methanol (12 mL) to make a clear solution, and $Na_2S_2O_4$ (841 mg, 4.83 mmol) was added. Water (1.2 mL) was added, and the reaction mixture was stirred in a sealed vial and heated at 115 °C for 4 h. The reaction mixture was then cooled to 23 °C, and solvent was removed. The residue was dissolved in dichloromethane (27 mL) and filtered to remove the solid. Dichloromethane was evaporated to afford a crude product **24** (566 mg). Without purification, the crude product **24** was dissolved in THF (15.8 mL). Triethylamine (0.70 mL, 5.02 mmol) and isobutyryl chloride (118 μL, 1.12 mmol) were added dropwise to the solution at 0 °C. The reaction mixture was stirred at 0 °C for 40 min, and then it was stirred at 23 °C for 40 min. The solvent was evaporated, and the residue was separated by silica gel flash chromatography, eluting with hexane−ethyl acetate 5:1, to afford product **28** as a clear oil (486 mg, total yield 78%): ^{1}H NMR (300 MHz, $CDCl_3$) δ 7.38−7.18 (m, 10 H), 6.33 (s, 1 H) 5.35 (s, 1 H), 5.31−5.19 (m, 4 H), 3.93−3.50 (m, 7 H), 2.49−2.38 (septet, J = 5.4 Hz, 1 H), 1.12 (s, 3 H), 1.10 (s, 3 H). 0.90−0.76 (m, 36 H), 0.05 - −0.10 (m, 24 H); ^{13}C NMR (75 MHz, $CDCl_3$) δ 176.5, 163.9, 161.7, 160.4, 137.2, 136.7, 128.4, 128.3, 128.2, 127.9, 94.8, 76.8, 74.7, 71.5, 68.8, 68.4, 64.6, 43.3, 35.6, 29.7, 26.1, 26.0, 19.7, 19.6, 18.4, 18.3, 18.2, 18.1, −4.0, −4.2, −4.4, −5.1, −5.3, −5.4; MS (ESI) 983 *m*/*z* (MH^+). Anal. Calcd for $C_{51}H_{90}N_4O_7Si_4$: C, 62.27; H, 9.22; N, 5.70. Found: C, 62.49; H, 9.06; N, 6.08.

***N*-2,4-Bis(benzyloxy)-6-(ribitylamino)pyrimidin-5-ylisobutyramide (29).** Compound **28** (164 mg, 0.167 mmol) was dissolved in THF (5.1 mL). HF−Py solution (2.05 mL) was added to the solution. The reaction mixture was stirred at 23 °C for 6 h. Then $NaHCO_3$ powder and its saturated aqueous solution were added to the reaction mixture to neutralize it to pH 7−8. The solution was extracted with $CHCl_3$ (3 × 35 mL). The extracts were combined and dried over Na_2SO_4 for 2 h. The mixture was filtered, and the solvent was removed. The residue was separated by silica gel flash chromatography, eluting with dichloromethane-ethanol 10:1, to

provide a semisolid product **29** (56 mg, 63.7%): ^{1}H NMR (300 MHz, CD_3OD) δ 7.33−7.16 (m, 10 H), 5.24 (s, 2 H) 5.19 (s, 2 H), 3.79−3.40 (m, 7 H), 2.56−2.47 (septet, J = 6.9 Hz, 1 H), 1.05 (s, 3 H), 1.03 (s, 3 H); ^{13}C NMR (75 MHz, CD_3OD) δ 181.0, 166.4, 163.6, 163.3, 138.6, 138.3, 129.4, 129.0, 128.9, 128.7, 94.7, 74.4, 74.3, 72.7, 70.0, 69.3, 64.7, 44.7, 36.2, 19.9; MS (ESI) m/z 527 (MH^+). Anal. Calcd for $C_{27}H_{34}N_4O_7$: C, 61.58; H, 6.51; N, 10.64. Found: C, 61.22; H, 6.43; N, 10.28.

***N*-6-(Ribitylamino)pyrimidine-2,4(1*H*,3*H*)-dione-5-ylisobutyramide (30).** Intermediate **29** (30 mg, 0.057 mmol) was added to methanol−water (7 mL, 0.7 mL) to make a solution. Then Pd/C (10%, 7.5 mg) was added to the solution. The reaction mixture was stirred under 1 atm of H_2 at 23 °C for 24 h. The reaction mixture was filtered to remove the Pd/C. The solvent was removed from the filtrate to provide a light yellow amorphous powder (18.7 mg, 95%): mp 184−185 °C; ^{1}H NMR (300 MHz, D_2O) δ 3.78−3.27 (m, 7 H), 2.53−2.48 (p, J = 7.0, 1 H), 1.01 (s, 3 H), 0.99 (s, 1 H); ^{13}C NMR (75 MHz, D_2O) δ 185.4, 165.0, 156.1, 153.8, 89.0, 74.7, 72.6, 64.9, 46.5, 37.3, 21.1; MS (ESI) m/z 347 (MH^+). Anal. Calcd for $C_{13}H_{22}N_4O_7 \cdot 1.4\ H_2O$: 42.02; H, 6.73; N, 15.08. Found: C, 42.28; H, 6.55; N, 15.03.

***N*-(2,4-Bis(benzyloxy)-6-[2,3,4,5-(*tert*-butyldimethylsilyl)ribitylamino]pyrimidin-5-ylpropionamide (31).** Compound **23** (510 mg, 0.541 mmol) was dissolved in methanol (10 mL) to make a clear solution, and $Na_2S_2O_4$ (715 mg, 4.12 mmol) was added. Water (1.0 mL) was added to the solution. The reaction mixture was stirred in a sealed vial at 0 °C for 4 h. The reaction mixture was then cooled to 23 °C, and the solvent was evaporated. The residue was dissolved in dichloromethane (25 mL) and filtered to remove the solid. Dichloromethane was evaporated to afford a crude product **24** (535 mg). Without purification, the crude product **24** was dissolved in THF (15.0 mL). Triethylamine (0.66 mL, 4.74 mmol) was added to this solution. Propionyl chloride (92.1 μL, 1.05 mmol) was added dropwise to the solution at 0 °C. The reaction mixture was stirred at 0 °C for 40 min, and then it was stirred at 23 °C for 40 min. The solvent was removed. The residue was separated by silica gel flash chromatography, eluting with hexane−ethyl acetate 5:1, to afford product **31** as a clear oil (427 mg, total yield 80.3%): ^{1}H NMR (300 MHz, $CDCl_3$) δ 7.36−7.21 (m, 10 H), 6.40 (s, 1 H) 5.37 (s, 1 H), 5.32−5.26 (m, 4 H), 3.94−3.53 (m, 7 H), 2.31−2.23 (q, J = 7.8 Hz, 2 H), 1.14−1.09 (t, J = 7.5 Hz, 3 H). 0.91−0.82 (m, 36 H), 0.08- −0.05 (m, 24 H); ^{13}C NMR (75 MHz, $CDCl_3$) δ 178.4, 173.6, 164.3, 163.0, 162.4, 162.1, 160.7, 137.5, 137.2, 136.9, 128.9, 128.7, 128.6, 128.4, 128.3, 95.1, 75.1, 72.0, 71.7, 69.3, 68.7, 68.5, 65.0, 43.7, 30.0, 26.5, 26.4, 25.3, 18.9, 18.7, 18.6, 18.5, 10.2, −3.6, −3.9, −4.0, −4.1, −4.6, −4.8, −5.0; MS (ESI) m/z 969 (MH^+). Anal. Calcd for $C_{50}H_{88}N_4O_7Si_4$: C, 61.94; H, 9.15; N, 5.78. Found: C, 61.67; H, 9.24; N, 6.15.

***N*-2,4-Bis(benzyloxy)-6-(ribitylamino)pyrimidin-5-ylpropionamide (32).** Compound **31** (176 mg, 0.179 mmol) was dissolved in THF (5.5 mL). HF−Py solution (2.17 mL) was added to the solution. The reaction mixture was stirred at 23 °C for 6 h. Then $NaHCO_3$ powder and its saturated aqueous solution were added to the reaction mixture to neutralize to pH 7−8. The solution was extracted with $CHCl_3$ (3 × 37 mL). The extracts were combined and dried over Na_2SO_4 for 2 h. The mixture was filtered, and the solvent was removed. The residue was separated by silica gel flash chromatography, eluting with dichloromethane−ethanol 10:1, to provide a semisolid product **32** (60 mg, 65%): ^{1}H NMR (300 MHz CD_3OD) δ 7.31−7.15 (m, 10 H), 5.22 (s, 2 H) 5.21 (s, 2 H), 3.78−3.39 (m, 7 H), 2.31−2.23 (q, J = 7.8 Hz, 2 H), 1.07−1.02 (t, J = 7.8 Hz, 3 H); ^{13}C NMR (75 MHz, CD_3OD) δ 178.3, 166.7, 164.0, 163.7, 139.0, 138.9, 129.8, 129.4, 129.0, 95.1, 74.8, 74.6, 73.3, 70.4, 69.6, 65.0, 45.2, 30.5, 10.73; MS (ESI) 513 (MH^+). Anal. Calcd for $C_{26}H_{32}N_4O_7$: 60.93; H, 6.29; N, 10.93. Found: C, 60.84; H, 6.29; N, 10.58.

***N*-6-(Ribitylamino)pyrimidine-2,4(1*H*,3*H*)-dion-5-ylpropionamide (33).** Compound **32** (40 mg, 0.078 mmol) was added to methanol−water (9.5 mL, 0.95 mL) to make a solution. Then Pd/C (10%, 10 mg) was added, and the reaction mixture was stirred under 1 atm H_2 at 23 °C for 24 h and then filtered to remove the Pd/C. The solvent was removed from the filtrate to provide a light yellow solid powder (23 mg, 92%): mp 126−127 °C; ^{1}H NMR (300 MHz, D_2O) δ 3.77−3.31 (m, 7 H), 2.31−2.23 (q, J = 7.8 Hz, 2 H), 1.00−0.95 (t, J = 7.5 Hz, 3 H); ^{13}C NMR (75 MHz, D_2O) δ 180.1, 163.0, 154.1, 151.7, 86.8, 72.6, 70.7, 62.7, 44.5, 29.0, 9.3; MS (ESI) MH^+ 333. Anal. Calcd for $C_{12}H_{20}N_4O_7$: 43.37; H, 6.07; N, 16.86. Found: C, 43.22; H, 5.71; N, 16.48.

TABLE 2. Enzymes Used in Kinetic Assays

enzyme	organism	specific activity (μM mg^{-1} h^{-1})	concn of enzyme in reaction mixture (μg mL^{-1})
lumazine synthases:	*M. tuberculosis*	1.1	30
	B. subtilis	5.1	2.0
	S. pombe	4.2	0.9
riboflavin synthase:	*E. coli*	11.6	1.0

Kinetic Assays. All assays were performed in 96-well microtiter plates using computer-controlled microplate reader. Enzymes used in kinetic assays are specified in Table 2.

Lumazine Synthase Assay. Assay mixtures with variable concentration of **1** contained 50 mM Tris hydrochloride, pH 7.0, 100 mM NaCl, 2% (v/v) DMSO, 5 mM dithiothreitol, 100 μM **2**, lumazine synthase, and **1** (3−150 μM) in a volume of 0.2 mL. Assay mixtures were prepared as follows. A solution (175 μL) containing 103 mM NaCl, 5.1 mM dithiothreitol, 114 μM **2**, and lumazine synthase in 51 mM Tris hydrochloride, pH 7.0 was added to 4 μL of inhibitor in 100% (v/v) DMSO (inhibitor concentration window, 0 − 300 μM) in a well of a 96-well microtiter plate. The reaction was started by adding 21 μL of a solution containing 103 mM NaCl, 5.1 mM dithiothreitol, and substrate **1** (30−1500 μM) in 51 mM Tris hydrochloride, pH 7.0. The formation of 6,7-dimethyl-8-ribityllumazine (**3**) was measured online for the period of 40 min at 27 °C at 408 nm ($\epsilon_{lumazine}$ = 10200 M^{-1} cm^{-1}).

For kinetic assays in phosphate buffer, Tris hydrochloride and NaCl in reaction mixtures were replaced by 100 mM K/Na-phosphate pH 7.0. All other assay parameters were the same as describe above.

Riboflavin Synthase Assay. Assay mixtures contained 100 mM K/Na-phosphate pH 7.0, 1% (v/v) DMSO, 5 mM dithiothreitol, enzyme, and variable concentrations of **3** (3−50 μM) in a volume of 0.2 mL. Assay mixtures were prepared as follows. A solution (175 μL) containing 5.1 mM dithiothreitol and riboflavin synthase in 103 mM K/Na-phosphate pH 7.0 was added to 5 μL of inhibitor in 40% (v/v) DMSO (inhibitor concentration window, 0−400 μM) in a well of a 96-well microtiter plate. The reaction was started by adding 21 μL of a solution containing 5.1 mM dithiothreitol, and substrate **3** (30−500 μM) in 103 mM K/Na-phosphate pH 7.0. The formation of riboflavin was measured online for the period of 40 min at 27 °C at 470 nm ($\epsilon_{riboflavin}$ = 9600 M^{-1} cm^{-1}).

Evaluation of Experimental Data. The velocity−substrate data were fitted for all inhibitor concentrations with a nonlinear regression method using the program DynaFit.[34] Different inhibition models were considered for the calculation. K_i and K_{is} values ± standard deviations were obtained from the fit under consideration of the most likely inhibition model as described earlier.[35]

Acknowledgment. This research was made possible by NIH Grant Nos. GM51469 and R21 NS053634, the Fonds der Chemischen Industrie, the Hans Fischer Gesellschaft, and the

(34) Kuzmic, P. *Anal. Biochem.* **1996**, *237*, 260−273.
(35) Cushman, M.; Jin, G.; Illarionov, B.; Fischer, M.; Ladenstein, R.; Bacher, A. *J. Org. Chem.* **2005**, *70*, 8162−8170.

Swedish Natural Science Research Council (Vetenskapsrådet). This research was conducted in a facility constructed with support from Research Facilities Improvement Program Grant No. C06-14499 from the National Center for Research Resources of the National Institutes of Health.

Supporting Information Available: ^{1}H NMR and ^{13}C NMR spectra, Lineweaver−Burk plots for the inhibition of *M. tuberculosis* lumazine synthase by compounds **27**, **30**, and **33**, the protein crystallization procedure, diffraction data collection, data collection and refinement statistics, and structure determination and refinement. This material is available free of charge via the Internet at http://pubs.acs.org.

JO702631A